

# Spectral Energetics in Polar Regions Using JRA-25 Dataset

Yasushi WATARAI

Terrestrial Environment Research Center  
University of Tsukuba, Japan

and

Hiroshi L. TANAKA

Frontier Research Center for Global Change, JAMSTEC, Japan  
Center for Computational Sciences  
University of Tsukuba, Japan

## 1. INTRODUCTION

Polar region is the sink of atmospheric energy and plays a major role in the global circulation. It is important to understand the role of polar regions within the global circulation and estimate the energy and energy transformation in these regions.

The global energy budget introduced by Lorenz (1955) gives a comprehensive view of the atmospheric circulation. Saltzman (1957, 1970) expanded it into zonal wavenumber domain. Many studies examined the global energy budget by use of these methods (e.g., Oort 1964; Manabe et al. 1970; Kung and Tanaka 1983). However, it is difficult to recognize the role of polar regions from the global-mean budget.

The purpose of this study is to examine the energy budget in polar regions by using the energy budget equations with zonal wavenumber domain. In order to estimate the energy budget, JRA-25 dataset, which is an up-to-date reanalysis data made in Japan, is used.

## 2. METHOD AND DATA

Energy cycle after Lorenz (1955) is a powerful tool to examine the aspect of general circulation. It is represented as the budget equations of available potential energy ( $P$ ) and kinetic energy ( $K$ ), divided between zonal and eddy components:

$$\frac{\partial P_Z}{\partial t} = G(P_Z) - R(P_Z, P_E) - C(P_Z, K_Z), \quad (1)$$

$$\frac{\partial P_E}{\partial t} = G(P_E) + R(P_Z, P_E) - C(P_E, K_E), \quad (2)$$

$$\frac{\partial K_Z}{\partial t} = M(K_E, K_Z) + C(P_Z, K_Z) - D(K_Z), \quad (3)$$

$$\frac{\partial K_E}{\partial t} = -M(K_E, K_Z) + C(P_E, K_E) - D(K_E). \quad (4)$$

Here, subscripts  $Z$  and  $E$  designate the zonal and eddy components, respectively.  $G$  is the generation of  $P$ ,  $R$  the conversion from  $P_Z$  to  $P_E$ ,  $M$  the conversion from  $K_E$  to  $K_Z$ ,  $C$  the conversion from  $P$  to  $K$ , and  $D$  the dissipation of  $K$ . All terms in Eqs. (1)-(4) represent the values integrated over the total mass of atmosphere.

Saltzman (1957, 1970) expanded it into the spectral energetics in terms of the Fourier decomposition in zonal direction. This scheme enables us to examine the mutual interactions between eddies. Equations for the eddy, Eqs. (2) and (4), can be rewritten as follows:

$$\frac{\partial P(n)}{\partial t} = G(n) + R(n) + S(n) - C(n), \quad (5)$$

$$\frac{\partial K(n)}{\partial t} = -M(n) + L(n) + C(n) - D(n), \quad (6)$$

at  $N = 1, 2, 3, \dots, N$ . Here  $n$  is the zonal wave number. In Eqs. (5) and (6),  $R(n)$  and  $-M(n)$  represent the conversion from zonal component to the eddy of zonal wave number  $n$  (i.e., zonal-wave interactions) in available potential energy and kinetic energy, respectively. Their terms satisfy  $R(P_Z, P_E) = \sum_{n=1}^{\infty} R(n)$  and  $M(K_E, K_Z) = \sum_{n=1}^{\infty} M(n)$ . Wave-wave interactions of available potential energy and ki-

Saltzman Cycle

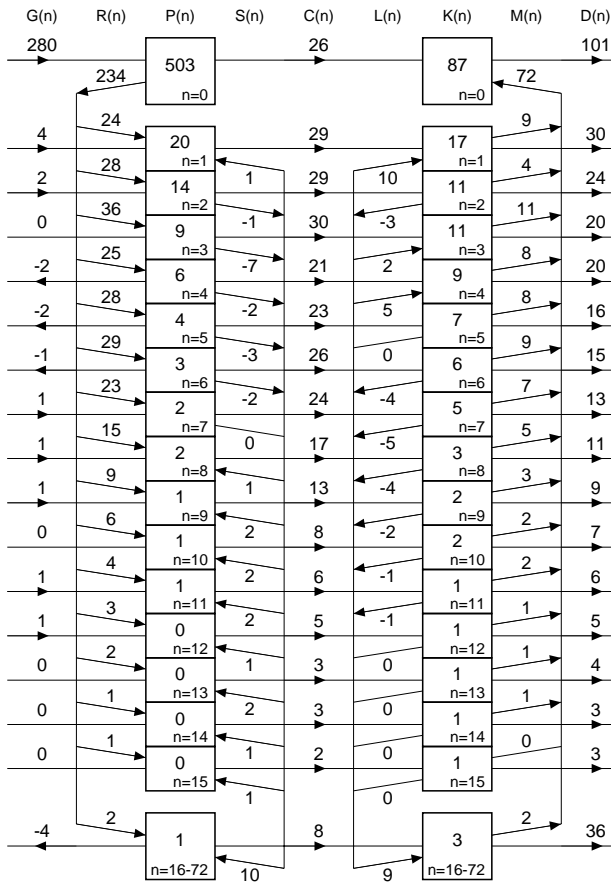


Figure 1: Energy flow diagram in the zonal wavenumber domain for 22 winters from 1979 to 2000 with JRA-25 dataset. Units of energy and transformation are  $10^4 \text{ Jm}^{-2}$  and  $10^{-2} \text{ Wm}^{-2}$ , respectively.

netic energy are designated by  $S(n)$  and  $L(n)$ , which show the energy conversion from all eddies to the eddy whose zonal wave number is  $n$ . The total sum of  $S$  ( $L$ ) is zero; i.e.,  $\sum_{n=1}^{\infty} S(n) = 0$  and  $\sum_{n=1}^{\infty} L(n) = 0$ . In this study,  $N$  in Eqs. (5) and (6) is set at 72, which is the Nyquist wave number.

The data used in this study are six-hourly JRA-25 dataset for 22 winters (DJF) from 1979 to 2000. It was downloaded from the JRA-25 homepage (<http://www.jreap.org/>). Resolution of given data is  $2.5^\circ \times 2.5^\circ$  intervals in longitude/latitude directions and 23 vertical levels (1000, 925, 850, 700, 600, 500, 400, 300, 250, 200, 150, 100, 70, 50, 30, 20, 10, 7, 5, 3, 2, 1 and 0.4 hPa). Field variables used for computing the energy cycle are the horizontal wind,  $(u, v)$ , temperature,  $T$ , and dew-point depression,  $T - T_d$ .  $T - T_d$  is available in 8 levels up to 300 hPa.

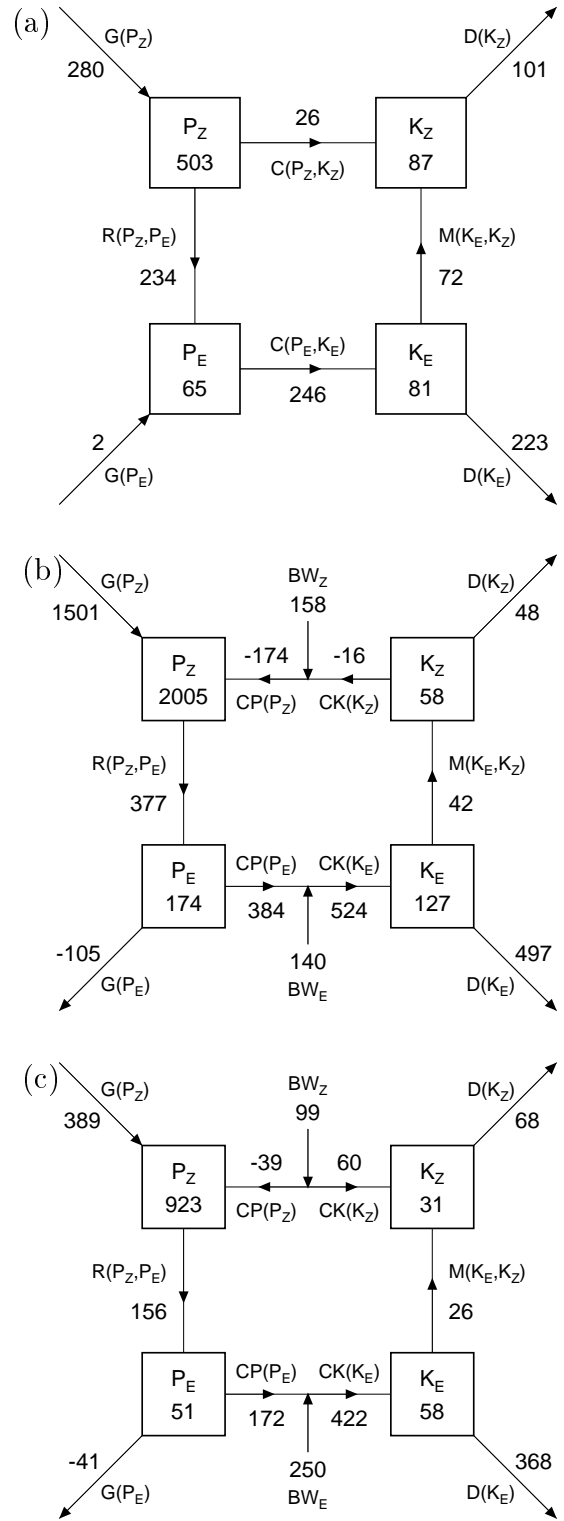


Figure 2: Energy box diagram in (a) global, (b) north polar and (c) south polar region, for 22 winters from 1979 to 2000 with JRA-25 dataset. Units of energy and transformation are  $10^4 \text{ Jm}^{-2}$  and  $10^{-2} \text{ Wm}^{-2}$ , respectively.

### 3. RESULT

First, global-mean energy budgets were estimated by use of JRA-25 dataset. Figure 1 shows the diagram of global-mean energy flows averaged for 22 winters from 1979 to 2000. Large  $G(0)$  ( $2.80 \text{ Wm}^{-2}$ ) due to differential heating is most of the energy input into the global energy cycle. Zonal available potential energy  $P(0)$  is converted to eddy available potential energy  $P(n)$  via  $R(n)$ , and  $P(n)$  is converted to eddy kinetic energy  $K(n)$  via  $C(n)$ . The peak of  $R(n)$  and  $C(n)$  is zonal wavenumber 3, and another peak is seen in zonal wavenumber 6. Wave-wave interactions,  $S(n)$  and  $L(n)$ , redistribute  $P(n)$  and  $K(n)$  among the eddy components. The directions of  $S(n)$  show that the available potential energies of  $n = 2$  to 6 are converted to higher frequency eddies ( $n \geq 8$ ). On the other hand,  $L(n)$  converts the synoptic-scale eddies ( $n = 6$  to 11) to both downscale and upscale. The energy input into  $K(n)$  is mostly balanced with dissipation  $D(n)$ , and partly converted to zonal kinetic energy  $K(0)$  via  $M(n)$ . Zonal-mean meridional circulation makes the conversion from  $P(0)$  to  $K(0)$ , i.e.  $C(0)$ , and the magnitude of  $C(0)$  is about 10 % of  $R(n)$ .

Next, we examine the energy budget of polar regions in the same manner. North and south polar regions are defined as  $60\text{-}90^\circ\text{N}$  and  $60\text{-}90^\circ\text{S}$ , respectively. Figure 2 illustrates four-box diagrams of energy flows in (a) global-mean, (b) north polar and (c) south polar region. In the north polar region, the magnitudes of  $P_Z$ ,  $P_E$ ,  $K_Z$  and  $K_E$  are 2005, 174, 58 and  $127 \times 10^4 \text{ Jm}^{-2}$ , which are about 400, 270, 70 and 160 % of the global mean. These are 923, 51, 31 and  $58 \times 10^4 \text{ Jm}^{-2}$  in the south polar region, which are about 180, 80, 40 and 70 % of the global mean. It is natural that  $P_Z$  in the polar regions is much larger than in the global mean, since the available potential energy introduced by Lorenz (1955) is proportional to the square of temperature deviation from the zonal and meridional averages. The value of  $K_Z$  in the polar regions is small in comparison with the global mean. It seems that the small  $K_Z$  is due to the jet stream out of the defined polar regions. Overall, the energy components in the south polar region is a half of the north polar region. It is suggested that its characteristic is mainly due to the difference of season.

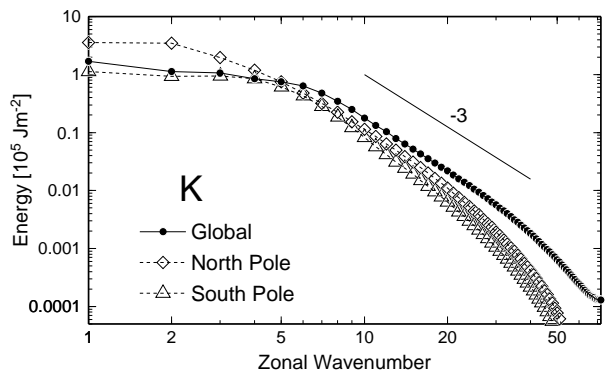


Figure 3: Energy spectra in the zonal wavenumber domain for 22 winters from 1979 to 2000 with JRA-25 dataset.

In Fig. 2(b),  $K_E$  is about 60 % larger than the value in the global mean. In order to examine the feature for each zonal wavenumber, the energy spectra of kinetic energy are showed in Fig. 3. Energy spectrum in the north polar region is larger than the global mean in low-frequency waves (zonal wavenumber 1-5). In contrast, high-frequency components (zonal wavenumber  $\geq 6$ ) show small energy in the north polar region in comparison with in the global mean. These results suggest that planetary waves are dominant in the polar regions. In south polar region, kinetic energy is smaller than in the global mean in all the wavenumbers.

When the energy budget is evaluated into the limited region, we must consider the energy flows through the boundaries of the region. Now we study the zonal baroclinic conversion  $C(0)$ . In the energy budget equations averaged over the polar region, the conversion of available potential energy released within the region to kinetic energy either within or outside the region,  $CP(P_Z)$ , is written by

$$CP(P_Z) = - \int \frac{R}{p} \bar{T} \bar{\omega}, \quad (7)$$

where the bar denotes the zonal average,  $\int$  the average over the polar region,  $p$  the pressure,  $T$  the temperature,  $\omega$  the vertical  $p$ -velocity and  $R$  the gas constant for air. On the other hand, the conversion of available potential energy released either within or outside of the region to kinetic energy within the region,  $CK(K_Z)$ , is written by

$$CK(K_Z) = - \int \bar{\mathbf{v}} \cdot \nabla \bar{\Phi}, \quad (8)$$

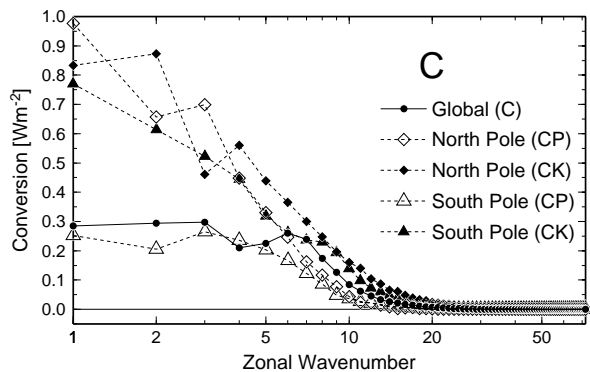


Figure 4: Conversion from eddy available potential energy to eddy kinetic energy for 22 winters from 1979 to 2000 with JRA-25 dataset. In polar regions, both  $CP$  and  $CK$  are shown.

where  $\mathbf{V} = (u, v)$  shows the horizontal wind and  $\Phi$  denotes the geopotential. Therefore,  $CK(K_Z)$  and  $CP(P_Z)$  are related by

$$CK(K_Z) - CP(P_Z) = - \int \frac{1}{a \cos \theta} \frac{\partial \bar{v} \bar{\Phi} \cos \theta}{\partial \theta} \equiv BW_Z, \quad (9)$$

where  $a$  is the radius of the earth.  $BW_Z$  is the work of the pressure gradient on the boundary. This term vanishes when it is integrated over the total mass of the atmosphere. Eddy component  $C(n)$  is represented the following

$$CK(n) - CP(n) = BW(n), \quad n = 1, 2, 3, \dots, \quad (10)$$

as well as  $C(0)$ .

In Figs. 2(b,c), terms of  $CP$ ,  $CK$  and  $BW$  are shown. In both polar regions,  $CP$  is not correspondent to  $CK$  and positive  $BW$  largely contributes to  $C$  in both zonal and eddy components. It is suggested that the conversion from available potential energy to kinetic energy in the polar region is largely affected the inflow of potential energy from the midlatitude. Figure 4 shows the spectra of  $C(n)$ . Both  $CP$  and  $CK$  are shown in polar regions. In north polar region,  $CK$  is larger than  $CP$  in almost all wavenumbers, which represents the positive  $BW$ . However,  $CP > CK$  and negative  $BW$  are shown in zonal wavenumbers 1 and 3. It suggests the dominance of these wavenumbers (i.e. planetary waves) in the north polar region. In south polar region,  $CK$  is about twice of  $CP$  in all wavenumbers, which indicates larger contribution from midlatitude.

## 4. SUMMARY

In this study, energetics analysis in the zonal wavenumber domain is conducted for the global mean and polar regions, by use of the JRA-25 dataset which is an up-to-date reanalysis made in Japan. Climatological characteristics for the boreal winter (DJF) of 1979-2000 are examined.

In the north polar region, the magnitudes of  $P_Z$ ,  $P_E$ ,  $K_Z$  and  $K_E$  are about 400, 270, 70 and 160 % of the global mean. The energy components in the south polar region are very small in comparison with the global mean or the north polar region. The conversion from available potential energy to kinetic energy is largely affected by the cross-boundary flux from the midlatitude, as well as the conversion within the polar region. In the north polar region, kinetic energy in low-frequency eddies is fairly large and  $BW$  is negative in the zonal wavenumbers 1 and 3, which suggests the importance of planetary waves in the north polar region.

## Acknowledgments

The JRA-25 datasets used for this study are provided from the cooperative research project of the JRA-25 long-term reanalysis by Japan Meteorological Agency (JMA) and Central Research Institute of Electric Power Industry (CRIEPI). All figures are drawn by the Generic Mapping Tools (GMT) graphics (Wessel and Smith 1991).

## REFERENCES

- Kung, E. C. and H. Tanaka, 1983: Energetics analysis of the global circulation during the special observation periods of FGGE. *J. Atmos. Sci.*, **40**, 2575–2592.
- Lorenz, E. N., 1955: Available potential energy and the maintenance of the general circulation. *Tellus*, **7**, 157–167.
- Manabe, S., J. Smagorinsky, J. L. Holloway, Jr. and H. M. Stone, 1970: Simulated climatology of a general circulation model with a hydrologic cycle: III. Effects of increased horizontal computational resolution. *Mon. Wea. Rev.*, **98**, 175–212.
- Oort, A. H., 1964: On estimates of the atmospheric energy cycle. *Mon. Wea. Rev.*, **92**, 483–493.
- Saltzman, B., 1957: Equations governing the energetics of the larger scales of atmospheric turbulence in the domain of wave number. *J. Meteor.*, **14**, 513–523.
- Saltzman, B., 1970: Large-scale atmospheric energetics in the wave-number domain. *Rev. Geophys. Space Phys.*, **8**, 289–302.
- Wessel, P. and W. H. F. Smith, 1991: Free software helps map and display data. *EOS Trans. Amer. Geophys. U.*, **72**, 441, 445–446.